

Multiple-order Raman scattering by a localized mode

T. P. Martin

Max-Planck-Institut für Festkörperforschung, Stuttgart 80, Federal Republic of Germany

(Received 8 September 1975)

Resonant Raman scattering, up to seventeenth order, was observed in additively colored CsI. The Raman spectrum is dominated by a series of sharp, intense, equally spaced lines due to a localized mode associated with the defect. The principal mechanism for broadening of these lines is shown to be the anharmonic decay of the localized mode into two band modes. For the case of anharmonically broadened lines, a criterion is established to distinguish between hot luminescence and resonant Raman scattering. Each of the sharp lines exhibits a side band which resembles the phonon density of states of pure CsI. The intensity of the side bands is relatively constant out to tenth order even though the intensity of the main line decreases as $(\text{order})^{-1}$. This behavior can be simply explained by the multiplicity of scattering diagrams.

INTRODUCTION

Because of the inversion symmetry of all atoms in pure CsI, Raman scattering of first order is not allowed. Defects destroy this symmetry, permitting first- and higher-order Raman scattering from a large sampling of modes throughout the Brillouin zone. If the defect has a dipole active electronic transition with energy near the laser frequency, processes described as impurity-induced resonant Raman scattering or hot luminescence might be expected. If, in addition, the defect has a localized mode, scattering from this mode should be particularly important near resonance owing to the strong electron-phonon coupling between the localized vibration and the localized electronic state. Impurity-induced Raman scattering has been previously observed in both resonant^{1,2} and nonresonant systems.³ In a previous paper,¹ the temperature dependence and the laser frequency dependence of up to sixth-order Raman scattering by a localized mode in additively colored CsI have been reported and discussed. Now, by optimizing experimental conditions, i. e., defect concentration, sample temperature, and laser frequency, we are able to observe Raman scattering up to seventeenth order. Associated with each of the Raman lines is a side band resembling the density of states of pure CsI. Phonon side bands are well-known phenomena in normal luminescence processes. Such vibronic structure has been seen in both insulators⁴ and semiconductors.⁵ In the present paper, side bands of multiple-order Raman scattering lines are reported and discussed.

EXPERIMENT

The crystals used in this experiment were grown from the melt in a 500-Torr atmosphere of HI. We believe the resulting color centers to be I_3^- . Normally, such a color center would be unstable at room temperature in most alkali halides.

However, since the polyhalide CsI_3 can be produced at standard temperature and pressure,⁶ it is not unreasonable to expect that the I_3^- center is stable in CsI. Furthermore, I_3^- in solution is known⁷ to have a characteristic Raman-active mode at 110 cm^{-1} , almost exactly the frequency of the localized mode reported here.

The Raman measurements were made using a Jarrel-Ash double monochromator with photon counting detection. Measurement at low temperature was necessitated by the unusual property that the integrated intensity of the secondary radiation increased with decreasing temperature. We know from previous measurements that the peak resonant enhancement of the Raman intensity occurs for $5582\text{-}\text{\AA}$ laser radiation if the sample is at room temperature. With the sample at 8°K , the intensity was highest for the laser line with shortest available wavelength, 4579 \AA .

RESULTS AND DISCUSSION

Figure 1 shows a Raman spectrum of additively colored CsI cooled to 8°K . The spectrum consists of 17 equally spaced lines each exhibiting a weak side band. Within the accuracy of the experiment, the strong lines occur at multiples of the fundamental frequency 111 cm^{-1} . Since the maximum phonon frequency in pure CsI is 80 cm^{-1} , the scattering must involve a localized mode. This mode probably resembles the symmetric stretching mode of the linear I_3^- ion in solution.⁷ Of primary interest in this paper is the occurrence of side bands which can be seen to suffer little attenuation from zeroth to tenth order. Figure 2 compares the frequency dependence of the side band with a calculated density of states of pure CsI having its frequency origin at the center of the associated localized mode line. The side-band spectrum measured at 8°K is shifted to higher frequencies compared to the calculated density of states curve based on room-temperature neutron

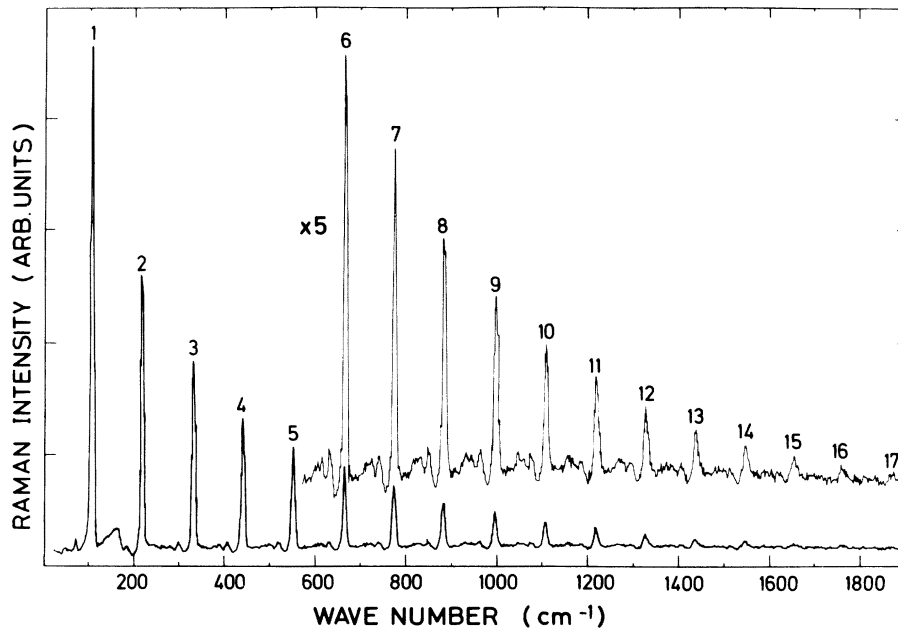


FIG. 1. Raman scattering spectrum of additively colored CsI measured at 8°K with the 4579-Å Ar line. The 17 equally spaced lines are multiple-order scattering from a localized mode. Each of these strong lines exhibits a side band.

scattering data.⁸ This shift is just that expected from the known⁹ temperature dependence of the reststrahl frequency.

There has been considerable controversy in the past few years as to whether or not resonant Raman scattering and hot luminescence are distinguishable phenomena.¹⁰⁻¹² Since we will find it convenient to use these terms to describe distinct phenomena, a word of explanation is in order. We assume we are dealing with a localized system with a strong electron-phonon interaction. In this case, it is convenient to calculate the eigenvalues and eigenvectors of the interacting electron-phonon system before applying the electromagnetic field. The energy levels of such a system are shown schematically in Fig. 3. Here, we have shown various vibrational levels of both the ground and excited electronic state. The number of quanta in the localized mode is given by N , the number in a typical band mode by n . Due to the electron phonon interaction, dipole transition between ground and the excited states with differing vibrational quantum number are allowed. In addition, we must consider the possibility of anharmonic decay of a highly excited localized mode into band modes. It is the presence of this additional anharmonic process which, by our definition, distinguishes hot luminescence from resonant Raman scattering. That is, as depicted in Fig. 3, hot luminescence arises from the emission of a photon after one or more quanta of vibrational energy have been lost through anharmonic decay. Resonant Raman scattering arises from the creation or destruction of a phonon in the ground electronic state following virtual excitation.

The question now arises: What is the mechanism for the observed series of sharp lines, resonant Raman scattering, or hot luminescence? In principle, this question can be answered by considering the order dependence of either the intensities or the widths of the localized mode lines. In practice, a study of the linewidths offers a much simpler criterion for distinguishing between the two processes.

Width of localized mode lines

One mechanism for the broadening of a localized mode is its anharmonic decay into band

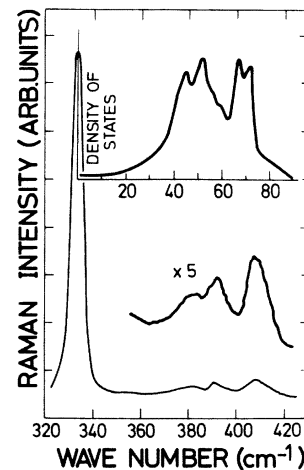


FIG. 2. Raman spectrum of additively colored CsI measured at 8°K with high signal to noise in the frequency region near the third-order peak. The upper curve shows the calculated phonon density of states based on room-temperature neutron scattering data (Ref. 8).

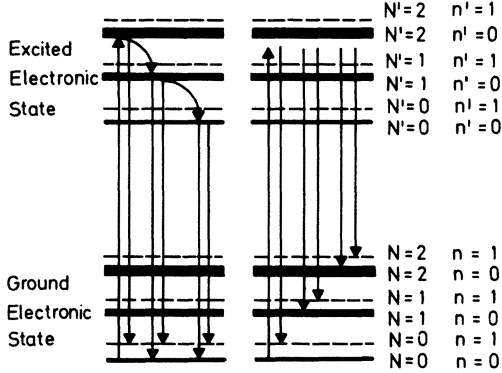


FIG. 3. Schematic representation of the energy levels and transitions in a strongly coupled electron-phonon system. The quantum number of the localized mode and one typical band mode are indicated by n and N , respectively. The straight lines indicate dipole transitions and the curved lines anharmonic phonon decay. The width of the localized mode state is shown to increase linearly with N or N' . The processes on the left-hand side represent hot luminescence, those on the right-hand side represent resonant Raman scattering.

modes resembling traveling waves.^{13,14} The energy of the localized mode in the CsI system is low enough to allow its decay into only two band modes. Such a three phonon process results from cubic anharmonicity. The appropriate Hamiltonian can be written

$$H_3 = \frac{1}{6} \left(\frac{\hbar^3 V}{8} \right)^{1/2} \sum_{kk'} (A + A^\dagger) [a(k) + a^\dagger(k)] \times [a(k') + a^\dagger(k')] \phi_{kk'} [\Omega \omega(k) \omega(k')]^{-1/2}, \quad (1)$$

where $a(k)$, $a^\dagger(k)$, and $\omega(k)$ are the annihilation operator, creation operator, and eigenfrequency of band mode k . The capital letters A , A^\dagger , Ω are the corresponding quantities of the localized mode. The volume of a unit cell has been denoted by V . This Hamiltonian is not very practical for computation since there is a different anharmonic coefficient $\phi_{kk'}$ for each pair of band modes. Therefore, we assume the anharmonic coupling is proportional to ω ,

$$\phi_{kk'} = \Phi_0 \omega(k) \omega(k'). \quad (2)$$

Such an approximation holds within the Debye model if $\phi_{kk'}$ is proportional to strain.¹⁴ Using standard second-order perturbation theory, this Hamiltonian leads to an inverse relaxation time given by

$$\frac{1}{\tau} = \frac{\pi \hbar V \Phi_0}{144 \Omega} N \sum_{kk'} \omega(k) \omega(k') \times [n(k) + n(k') + 1] \delta(\omega(k) + \omega(k') - \Omega). \quad (3)$$

The number of quanta in the localized mode and

in the k th mode have been written N and $n(k)$, respectively. Using the temperature dependence of $n(k)$,

$$n(k) = (e^{\hbar \omega / kT} - 1)^{-1}, \quad (4)$$

the low-temperature limit of Eq. (3) becomes

$$\frac{1}{\tau} \rightarrow \frac{\pi \hbar V \Phi_0 N}{144 \Omega} \sum_{kk'} \omega(k) \omega(k') \delta(\omega(k) + \omega(k') - \Omega), \quad (5)$$

and the high-temperature limit

$$\frac{1}{\tau} \rightarrow \frac{\pi V \Phi_0 N}{144} kT \sum_{kk'} \delta(\omega(k) + \omega(k') - \Omega). \quad (6)$$

At low temperatures the linewidth of the localized mode should be independent of temperature, at high temperatures a linear dependence is expected.

The summations can be performed using the known density of states⁸ determined from neutron-scattering experiments. The only unknown parameter is Φ_0 which can be fixed by the measured low-temperature value of the half width. No additional parameters are needed to determine the slope of the curve at high temperature. Comparison with experiment is made in Fig. 4. Here, we have plotted the temperature dependence of the width of the first-order line including a correction for the instrumental broadening. The agreement between the calculated and measured values is good. Therefore, we conclude that the broadening of the localized mode lines is due to anharmonic decay into two band modes.

We are now in a position to establish a criterion for distinguishing between resonant Raman scattering and hot luminescence. Equation (3) indicates that the anharmonic width of a localized mode state with N quanta of energy is N times that of a state with one quantum. The relative widths of several states are shown in Fig. 3. For the

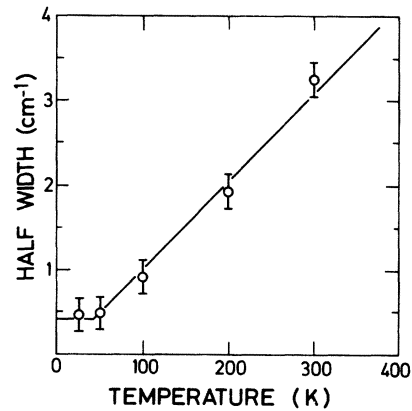


FIG. 4. Measured temperature dependence of the half-width of the first-order localized mode line at 111 cm^{-1} . The solid line segments indicate the calculated behavior for the low- and high-temperature limits.

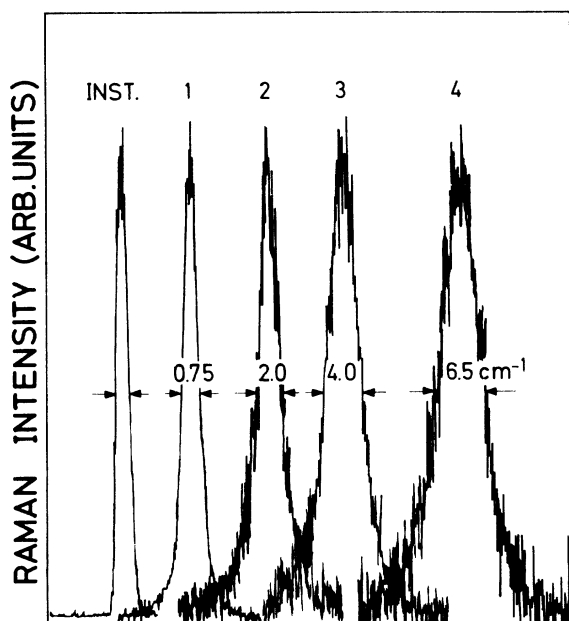


FIG. 5. Line shapes of the first four orders of Raman scattering from the localized mode. The instrumental profile is also shown. The numbers indicate the half-width after correcting for instrumental broadening.

hot luminescence processes, the spectral widths of the emitted radiation would be expected to decrease with order. That is, lines positioned far from the laser frequency will be narrower than lines close to the laser frequency. Just the reverse is expected for resonant Raman scattering. The observed order dependence of the line shape is shown in Fig. 5. In order to improve the instrumental resolution, these measurements were made with the 4880 laser line and with 80- μm slits. The anharmonic broadening was increased to a more easily measured value by raising the sample temperature to 110 $^{\circ}\text{K}$. Under these conditions, only the first four orders could be conveniently observed. Clearly, the linewidth increases with order. After subtracting the instrumental broadening this increase seems to be even greater than the first power of N . We conclude from this result that the secondary radiation observed in this sample is resonant Raman scattering and not hot luminescence.

Side bands

Figure 2 shows that the side-band spectrum strongly resembles the unweighted density of states of pure CsI if we assume that a given side band is associated with a localized mode which is closer in frequency to the laser line than is the side band itself. The intensity of the side bands falls off much more slowly with order than the intensity of the local mode lines. This can be

seen qualitatively in Fig. 1. The side band of the tenth-order line has about 50% of the intensity of the side band of the second-order line while the intensity of the localized mode line itself decreases by a factor of 8. We should mention that the structure in the spectrum near 170 cm^{-1} is not a side band but second-order Raman scattering from pure CsI. This additional scattering makes it difficult to define the first-order side band. The intensities of both the local mode lines and the side bands increase with decreasing temperature. Such behavior is not normally associated with Raman scattering. Detailed measurements of the temperature dependence of the localized mode lines have been presented in Ref. 1. Because of the weak signals, we have not been able to determine the functional dependence of the side-band intensity on temperature.

Two mechanisms are capable of producing side bands having the properties listed above. An anharmonic side band can be described by Raman processes, each with an additional intermediate state typically consisting of about n localized phonons. This intermediate state decays into a final state consists of n localized phonons plus a band mode. A similar mechanism has been successfully used to describe side bands of infrared absorption lines.¹⁵ This process is represented by diagram c in Fig. 6. The same cubic anharmonicity responsible for the width of the localized mode line is also responsible for the additional vertex in Fig. 6(c). The anharmonic coefficients are, however, not identical since the broadening process involves one localized mode phonon and two band mode phonons while the side band process involves two localized mode phonons and one band mode phonon. We might expect, however, that the magnitude of the two types of anharmonic coefficient will be the same. Using this assumption,

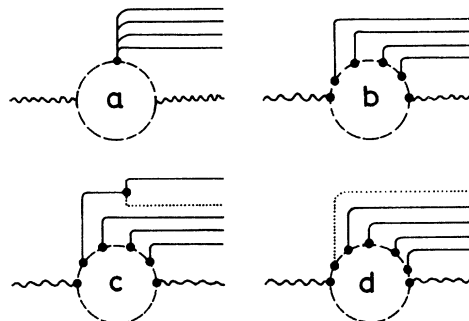


FIG. 6. Processes represented by a and b contribute to the main, fourth-order Raman line. Processes c and d contribute to the corresponding side band. The localized phonons are denoted with a solid line, the band phonons by a dotted line, the photons by a wavy line, and the electron-hole states by a broken line.

the calculated side band intensity can be shown to be several orders of magnitude smaller than the observed intensity, indicating that the side bands are probably not anharmonic in origin.

A Raman process with electronic coupling not only to the localized mode but to the band modes as well, would also result in side bands. Such a process is represented by diagram d in Fig. 6. This diagram offers a convenient explanation for side-band intensities which increase with order with respect to the corresponding localized mode-line intensities. For a process involving N identical localized phonons and one-band phonon, there exist $N+1$ nonequivalent diagrams. That is, the band mode vertex can occur between any of the localized mode vertices. The order dependence of the side band can be demonstrated more quantitatively by the following semiclassical argument. The Raman effect is due to a modulation of the electronic susceptibility χ by localized mode coordinates Q and band mode coordinates q . Expanding χ in a Taylor series, we obtain

$$\chi(Q, q) = \sum_{N,n} \frac{Q^N q^n}{N! n!} \frac{\partial^N}{\partial Q^N} \frac{\partial^n}{\partial q^n} \chi. \quad (7)$$

For a simple defect it is not unreasonable to assume that the susceptibility has the form

$$\chi = A(q, Q)/\omega_0(q, Q) - \omega. \quad (8)$$

In general, high-order derivatives of this expression will be rather complex. Near resonance, however, the term in the derivative with the highest power of the energy denominator will dominate. This approximation is equivalent to ignoring processes represented by diagram a in Fig. 6 and considering only processes represented by Fig. 6(b). Making this approximation,

$$\frac{\partial^N}{\partial Q^N} \frac{\partial^n}{\partial q^n} \chi \approx \frac{A(N+n)! (-1)^{N+n}}{(\omega_0 - \omega)^{N+n+1}} \left(\frac{\partial \omega_0}{\partial Q} \right)^N \left(\frac{\partial \omega_0}{\partial q} \right)^n, \quad (9)$$

and the intensity of Raman scattering becomes

$$I_{Nn} \sim \left| \frac{(N+n)!}{N! n!} \frac{A}{(\omega_0 - \omega)^{N+n+1}} \times \left(\frac{\partial \omega_0}{\partial Q} \right)^N \left(\frac{\partial \omega_0}{\partial q} \right)^n \right|^2 \langle Q^{2N} \rangle \langle q^{2n} \rangle. \quad (10)$$

In this notation, the intensity I_{N1} of the side band of the N th-order mode relative to the intensity of the main band I_{N0} becomes

$$\frac{I_{N1}}{I_{N0}} \approx \left| \frac{N+1}{\omega_0 - \omega} \left(\frac{\partial \omega_0}{\partial q} \right) \right|^2 \langle q^2 \rangle. \quad (11)$$

That is, the intensity of the side band increases relative to the main band as the order increases. The observed intensity dependence is not so strong as $(N+1)^2$ indicating that the assumptions made in Eqs. (8) and (9) do not strictly hold.

In a previous paper,¹ we presented measurements showing that the integrated Raman intensity increased with decreasing temperature. The explanation given in that paper was that there exists a nonradiative decay channel from the excited to the ground electronic state which is less effective at low temperature. This additional decay mechanism should also contribute appreciably to the line broadening. Since the line broadening has now been shown to be essentially anharmonic in origin, an alternative explanation of the temperature dependence must be found. Such an explanation becomes apparent if the configuration coordinate description of a localized electron-phonon interaction is considered. In this picture, increased Raman intensity will arise through an increase in the overlap integrals between the ground and excited state vibrational wave functions.¹⁶ This can be achieved by an increase in the lowest order electron-phonon interaction. Such an increase will also tend to raise the frequency for peak resonant enhancement. Examination of Fig. 3 in Ref. 1 shows that the laser frequency giving maximum Raman intensity did indeed shift from the yellow to the blue as the temperature of the sample is lowered.

In conclusion, two alternative mechanisms were considered to explain the series of sharp lines observed in the scattered radiation spectrum of additively colored CsI, resonant Raman scattering, and hot luminescence. Since the width of these lines was shown to be anharmonic in origin and to increase with order, we were able to conclude that resonant Raman scattering is the dominant mechanism. The density of states like side band associated with each sharp line is probably not anharmonic in origin but arises from a high-order electron-phonon interaction involving N localized phonons and one band mode.

ACKNOWLEDGMENTS

The crystals used in this experiment were grown by K. Bähr of the Physikalisches Institut der Universität Stuttgart. The author would like to thank M. Cardona, L. Genzel, and R. Zeyher for several stimulating conversations.

¹T. P. Martin, Phys. Rev. B **11**, 875 (1975).

²J. M. Worlock and S. P. S. Porto, Phys. Rev. Lett. **15**, 697 (1965); D. S. Pan and E. Lüty, Proceedings of

the International Conference on Light Scattering in Solids, 1975, (unpublished); C. J. Buchanauer, D. B. Fitchen and J. B. Page, in *Light Scattering Spectra of Solids*,

- edited by G. B. Wright (Springer, New York, 1969).
- ³A. Keil and J. B. Scott, *Phys. Rev. B* 2, 2033 (1970); R. T. Harley, J. B. Page, and C. T. Walker, *ibid.* 3, 1365 (1971).
- ⁴See, for example, D. L. Wood and W. Kaiser, *Phys. Rev.* 126, 2079 (1972); W. E. Bron and W. R. Heller, *ibid.* 136, A1433 (1964).
- ⁵D. G. Thomas and J. J. Hopfield, *Phys. Rev.* 128, 2135 (1962); Jagdeep Shah, R. L. Leheny, and A. H. Dayem, *Phys. Rev. Lett.* 33, 818 (1974); Jagdeep Shah, R. F. Leheny, and W. F. Brinkman, *Phys. Rev. B* 10, 659 (1974).
- ⁶A. I. Popov and R. E. Buckles, *Inorg. Syn.* 5, 167 (1957).
- ⁷W. Kiefer and H. J. Bernstein, *Chem. Phys. Lett.* 16, 5 (1972).
- ⁸W. Bührer and W. Hälg, *Phys. Status Solidi B* 46, 679 (1971).
- ⁹D. H. Martin, *Adv. Phys.* 14, 39 (1965).
- ¹⁰M. V. Klein, *Phys. Rev. B* 8, 919 (1973).
- ¹¹Y. R. Shen, *Phys. Rev. B* 9, 622 (1974).
- ¹²J. R. Solin and H. Merkelo, *Phys. Rev. B* 12, 624 (1975).
- ¹³P. G. Klemens, *Phys. Rev.* 122, 443 (1961).
- ¹⁴R. J. Elliott, W. Hayes, G. D. Jones, H. F. Macdonald, and C. T. Sennett, *Proc. R. Soc. A* 289, 1 (1965).
- ¹⁵B. Fritz, in *Proceedings of the 1963 International Conference on Lattice Dynamics* (Pergamon, London, 1964).
- ¹⁶P. P. Shorygin, *Sov. Phys.-Usp.* 16, 99 (1973).